Signal Detection and Timing Recovery for Two-Dimensional Magnetic Recording

Physical Nano-Memories Signal and Information Processing Laboratory

Chaitanya Kumar Matcha and Shayan Garani Srinivasa

Dept. of Electronic Systems Engg., Indian Institute of Science, Bengaluru.

Introduction

Two-dimensional magnetic recording (TDMR) is a promising technology for boosting areal densities using sophisticated signal processing algorithms within a systems framework. The channel impairments comprise of 2D inter-symbol interference (ISI), 2D synchronization errors along with media and electronic noise sources, making it challenging for designing optimum algorithms and architectures for read/write channels.

2D ISI detection is known to be NP-hard. This poses us a need to develop efficient as well as optimal detection algorithms to handle other channel impairments along with the 2D-ISI.

Voronoi media model of TDMR:

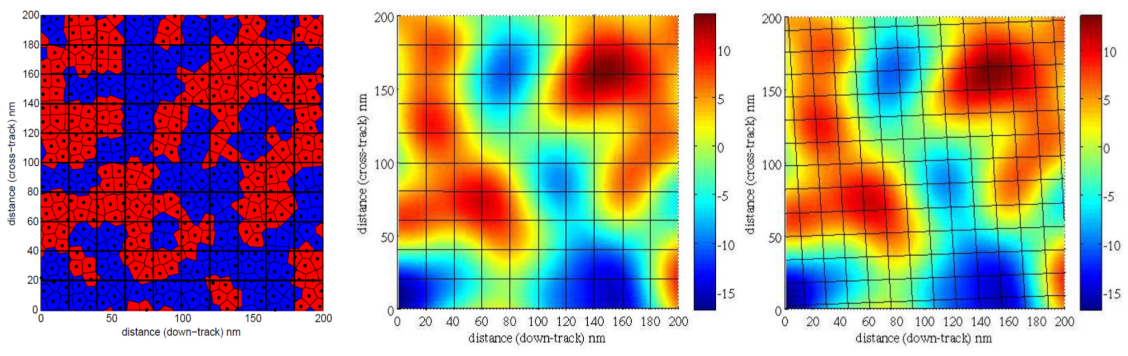

Magnetic grains are modelled as Voronoi regions. Grains are magnetized according to the bit-value. Each grain contributes to a Gaussian pulse.

(a) Ideal sampling. (b) Non-ideal sampling with frequency offsets.

Continuous-time readback signal is the contribution of all grains on the medium. The discrete-time samples are obtained by averaging over a bit-region centred at the sampling location.

2D Generalized Partial Response Target Design

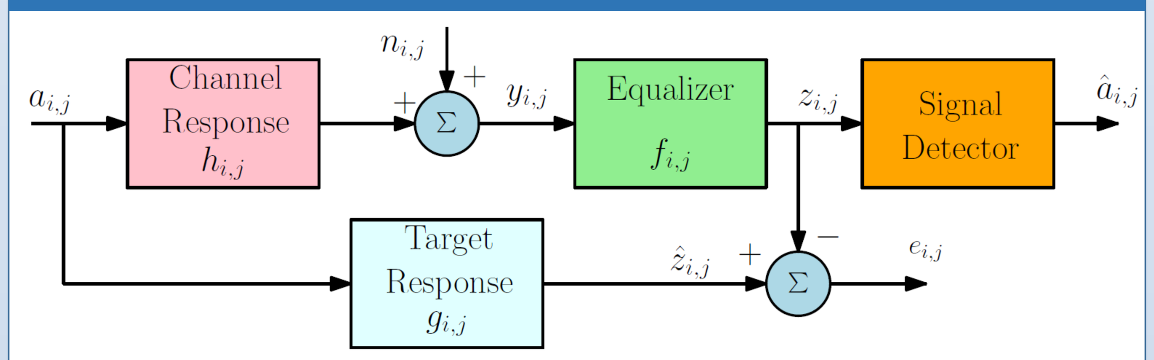

Signal received from the read channel is equalized using a linear equalizer to achieve a desired overall response called the partial response. The resultant signal is detected using a ML detector.

- GPR targets are widely used in conventional 1D magnetic recording
- Provides a trade-off between low-complexity linear equalizer and optimal ML detector.

MMSE based design of PR target and equalizer:

$$e_{i,j} = \underline{f}^T \underline{y}_F^{(i,j)} - \underline{g}^T \underline{a}_G^{(i,j)}$$

$$MSE = \mathbb{E}\left[\left|e_{i,j}\right|^2\right] = \underline{f}^T \boldsymbol{R}_{yy}\underline{f} + \underline{g}^T \boldsymbol{R}_{aa}\underline{g} - 2\underline{g}^T \boldsymbol{R}_{ay}\underline{f}$$

Solution:

- $\underline{f} = \boldsymbol{R}_{yy}{}^{-1}\boldsymbol{R}_{ay}{}^T \underline{g}$
- Monic constraint ($\underline{u}^T\underline{g} = 1$): $\underline{g} = \frac{\left(\boldsymbol{R}_{aa} - \boldsymbol{R}_{ay}\boldsymbol{R}_{yy}{}^{-1}\boldsymbol{R}_{ay}{}^T\right)^{-1}\underline{u}}{\underline{u}^T\left(\boldsymbol{R}_{aa} - \boldsymbol{R}_{ay}\boldsymbol{R}_{yy}{}^{-1}\boldsymbol{R}_{ay}{}^T\right)^{-1}\underline{u}}$
- Unit energy ($\underline{g}^T\underline{g} = 1$): $\underline{g} = \underline{v}_{min}$ of $\left(\boldsymbol{R}_{aa} - \boldsymbol{R}_{ay}\boldsymbol{R}_{yy}{}^{-1}\boldsymbol{R}_{ay}{}^T\right)$

Separable PR targets:

$$\boldsymbol{G} = \begin{bmatrix} g_{c0} \\ g_{c1} \\ g_{c2}\end{bmatrix}\begin{bmatrix} g_{r0} & g_{r1} & g_{r2}\end{bmatrix} = \begin{bmatrix} g_{c0}g_{r0} & g_{c1}g_{r0} & g_{c2}g_{r0} \\ g_{c0}g_{r1} & g_{c1}g_{r1} & g_{c2}g_{r1} \\ g_{c0}g_{r2} & g_{c1}g_{r2} & g_{c2}g_{r2}\end{bmatrix}$$

- Aids in detection using row-column detectors.
- Iterative optimization of g_r and g_c.

2D Soft-Output Viterbi Algorithm

2D ISI Detection - Background:

- 2D ISI detection is NP-Hard: ML detection is not practically feasible even for 64x64 page (512B sector).
- Trellis based algorithms: Use row-column detectors that exchange information in an iterative fashion.
- Graph based detector: Generalized belief propagation (GBP) algorithm uses message passing between regions instead of between nodes as in conventional BP algorithm.
- Performance of the 2D ISI detectors is not well understood.

2D Soft-output Viterbi Algorithm:

- Extend ideas of the 1D Viterbi algorithm.
- Make symbol decisions in raster scan order.
- Symbol decision is made by maximizing the likelihood probability of a local span ($\boldsymbol{M}$) of the readback samples.

$$Pr\left[\underline{y}_{\boldsymbol{M}}^{(i,j)} \middle| \{a_{m,n}\}_{m,n=-\infty}^{\infty}\right] \propto \exp\left(-\frac{1}{\sigma_w^2}\left\|\underline{y}_{\boldsymbol{M}}^{(i,j)} - \hat{\underline{y}}_{\boldsymbol{M}}^{(i,j)}\right\|^2\right),$$

where, $\hat{\underline{y}}_{\boldsymbol{M}}^{(i,j)} = \underline{g}^T \underline{a}_G^{(i,j)}$.

- ML Metric: $\Gamma^{(i,j)} = \left\|\underline{y}_{\boldsymbol{M}}^{(i,j)} - \hat{\underline{y}}_{\boldsymbol{M}}^{(i,j)}\right\|^2$
- Bit decision is made by minimizing ML metric

$$\hat{a}_{i,j} = \arg\min_{a_{i,j}} \Gamma^{(i,j)}$$

- Soft-ouput is obtained by identifying nearest alternative path with wrong decision:

$$LLR_{i,j} = \min_{a_{i,j}=1} \Gamma^{(i,j)} - \min_{a_{i,j}=-1} \Gamma^{(i,j)}$$

2D Data-Dependent Noise Prediction

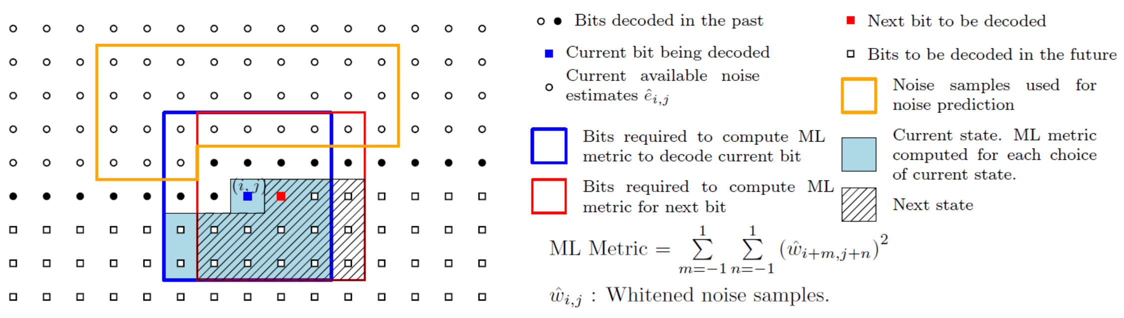

For 3x3 ISI, ML metric of a 3x3 span of received samples uses 5x5 span of bits. Out of these 25 bits, 12 bits are already detected in the raster scan order. 2^{13} ML metrics corresponding to the remaining 13 bits are computed to make the current bit-decision.

- Irregular bit-boundaries result in correlated media noise in the neighbouring positions.
- Noise depends on bit-transitions in crosstrack and downtrack directions results in data dependent media noise.
- Use linear noise prediction filters to decorrelate noise samples.
- Use data-dependent noise prediction filters to further handle media noise.

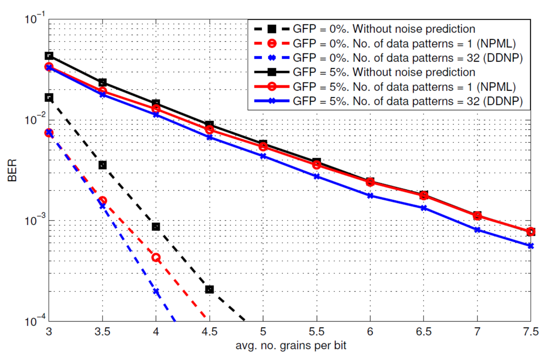

- 10% gain in areal density due to DDNP at 1.2 Tb/in^2
- Grain size = 10 nm.
- Bit-size = 22nm x 22 nm

2D Burst Erasure Correction

2D Burst Errors - Background:

- Thermal asperities result in burst erasures on the medium.
- Challenge is to correct 2D burst erasures of any shape.

Idea: Use metrics from 2D-SOVA to identify defective region. The erasure is indicated in the soft-information at the input of the LDPC decoder.

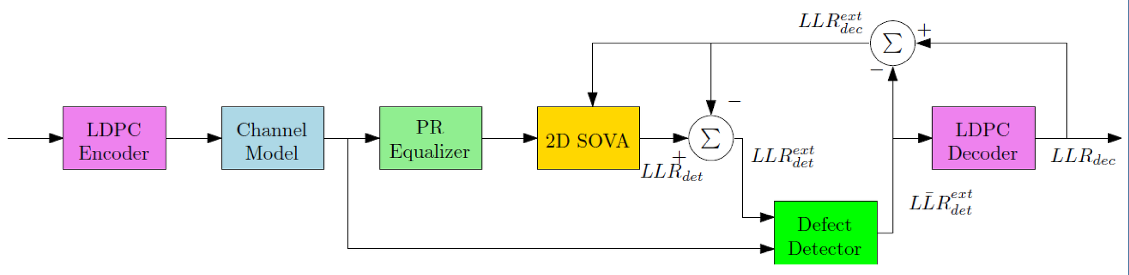

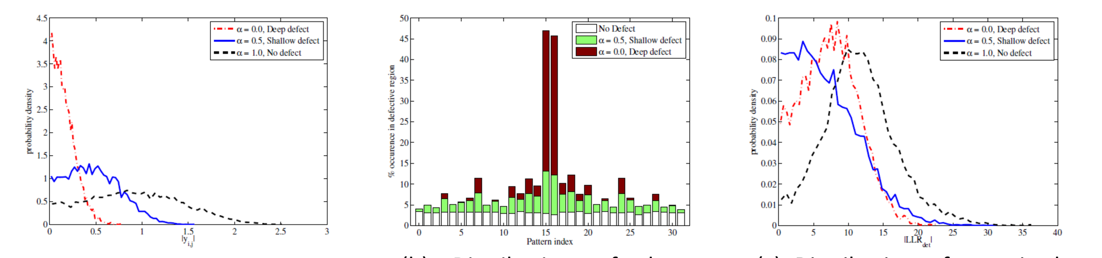

(a) Distribution of the readback sample magnitudes. The concentration of readback samples at low magnitude increases with the increase in the defect depth.

(b) Distribution of data patterns at detector's output. Certain data patterns occur often at the output of the detector within the defective region.

(c) Distribution of magnitude of LLRs at the output of 2D SOVA in defective and non-defective regions are compared.

- The readback signal strength is low in the defective region.
- Following bit-patterns are seen at the output of detector in the defective regions:

	0				1	
0	1	0		1	0	1
	0				1	

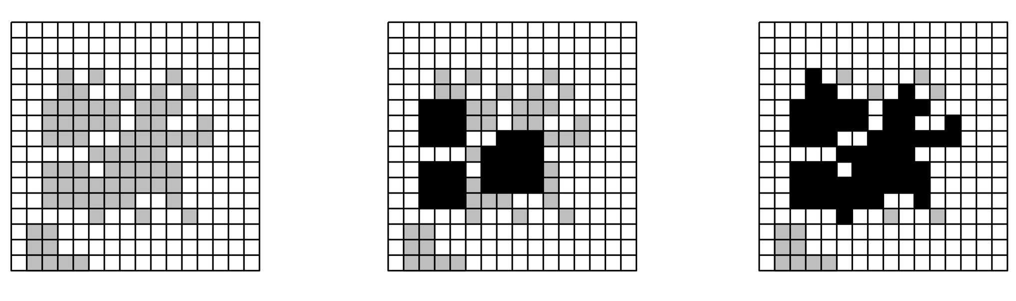

(a) Potentially defective regions identified by thresholding the readback signal as well as by identifying defective patterns at the output.

(b) Defective region identified as large (3x3) clusters.

(c) Defective region is further grown by extending to connected regions.

Defect detection and burst erasure correction:

- Identify potentially defective regions using
  - Threshold on readback signal
  - Identifying defective patter at the output of the detector.
- Defective regions are marked with at least 3x3 bursts.
- Defective region is grown to include connected regions.
- The soft-information corresponding to defective region is set 0 at the input of the LDPC decoder.

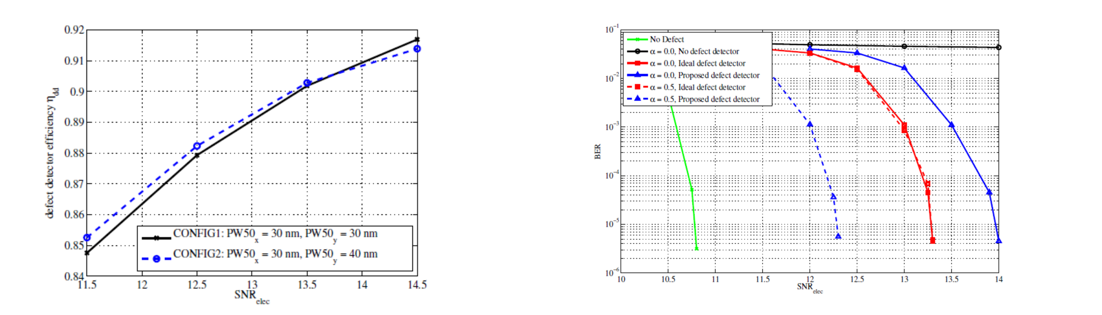

The proposed defect detector is observed to identify the defective region with >90% accuracy at the targeted SNR of 14.5 dB.

The proposed defect detector is able to perform better by 0.9dB than an ideal defect detector in the case of shallow defects ($\alpha = 0.5$) by ignoring only the erroneous information from 2D SOVA.

2D Joint Timing Recovery and Signal Detection

Sampling locations with 2D timing errors:

$$\begin{bmatrix}\tau_x(i,j)\\ \tau_y(i,j)\end{bmatrix} = \begin{bmatrix} jB_x \\ iB_y\end{bmatrix} + \begin{bmatrix} f_{xx} & f_{yx}\\ f_{xy} & f_{yy}\end{bmatrix}\begin{bmatrix} jB_x\\ iB_y\end{bmatrix} + \begin{bmatrix}\phi_x B_x\\ \phi_y B_y\end{bmatrix} + \begin{bmatrix}\theta_x(i,j)B_x\\ \theta_y(i,j)B_y\end{bmatrix}$$

Ideal location; Frequency offsets; Phase offsets; Jitter offsets

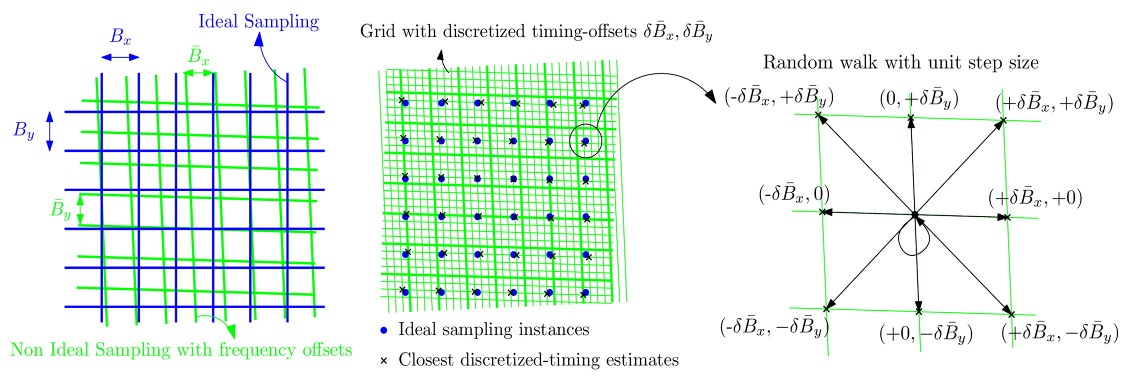

Signal is oversampled with unknown frequency offsets.

Timing offsets are discretized to a finer grid of size $\delta B_y \times \delta B_x$.

A 2D random walk of unit step results in 9 positions.

2D Random Walk Model:

- Timing estimates are discretized to multiples of δB_x and δB_y.
- The 2D joint timing recovery and signal detector uses 2D random walk model to estimate the timing error.

$$\delta\tau_x(i,j) \in \{0, \pm\delta B_x\}, \delta\tau_y(i,j) \in \{0, \pm\delta B_y\}$$

Joint 2D Interpolative Timing Recovery and Signal Detection

- Extends 2D SOVA to include timing information in the definition of the detector's state.
- Operates in the raster-scan order.
- Timing errors and bit-values are estimated by ML criterion for a local span of samples.
- Samples at estimated ideal locations are recovered using optimal interpolation filters.
- Optimal interpolation filters are design for every possible discrete time-offset using MMSE criterion.

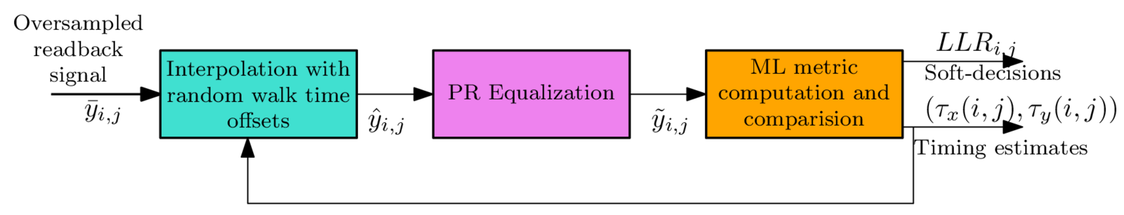

2D Iterative Timing Recovery Scheme

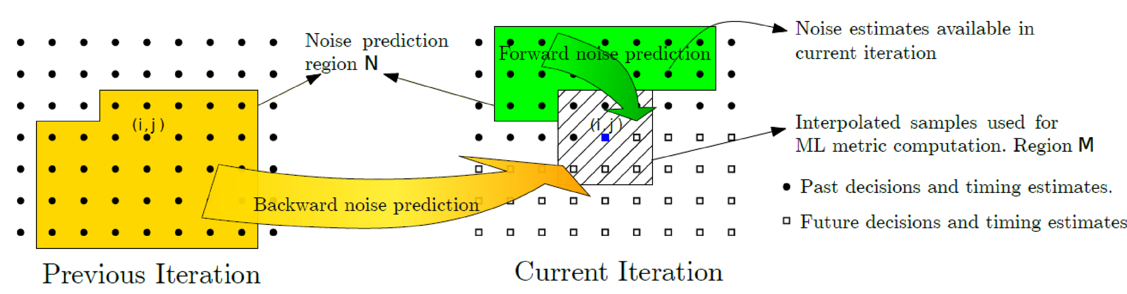

Raster scan order:

- Timing estimates of future bits are not available to estimate timing error for the current position.
- Only forward noise prediction can be done using the past decisions.

Iterative timing recovery scheme:

- Two instances of the joint timing-detection algorithm operating in different directions.
- The two detectors exchange extrinsic LLRs and timing estimates.

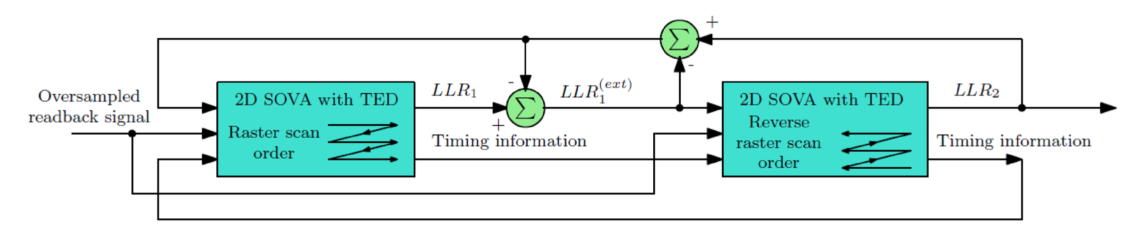

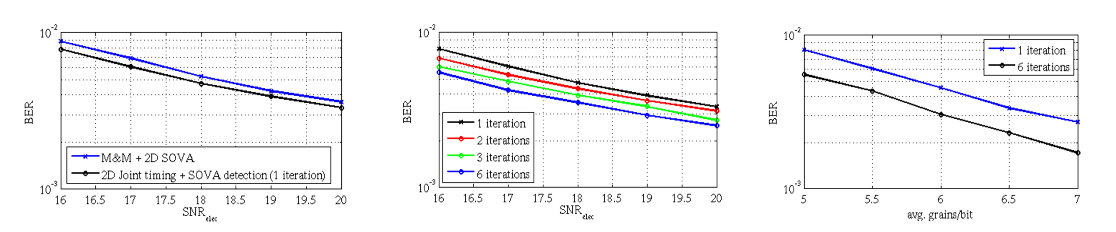

The proposed 2D joint timing recovery scheme performs better than 2D M&M based timing recovery scheme by 0.5 dB.

The 2D iterative timing recovery scheme gives > 1.2 dB gain in SNR over the open loop configuration.

2D iterative timing recovery scheme gives 10% gain in areal density over the open-loop configuration at 1 Tb/in^2.

References

Journals:

1. C. K. Matcha and S. G. Srinivasa, "Generalized Partial Response Equalization and Data Dependent Noise Predictive Signal Detection over Media Models for TDMR," *IEEE Trans. Magn.*, Oct. 2015.
2. C. K. Matcha and S. G. Srinivasa, "Defect Detection and Burst Erasure Correction for TDMR," *IEEE Trans. Magn.*, Nov. 2016.
3. C. K. Matcha and S. G. Srinivasa, "Joint Timing Recovery and Signal Detection for Two-dimensional Magnetic Recording," *IEEE Trans. Magn.*, Feb. 2017.

Patent:

1. S. G. Srinivasa, C. K. Matcha. A. Dey, "Method and Apparatus for Joint Adaptation of Two-dimensional Equalizer and Partial Response Target," *Indian patent (filed)*, Feb. 2017.

Signal Processing for Two-Dimensional Magnetic Recording Channels

Chaitanya Kumar Matcha and Shayan Garani Srinivasa

Department of Electronic Systems Engineering,
Indian Institute of Science, Bengaluru, 560012, India.

07-Apr-2017

Outline

Two-Dimensional Magnetic Recording

Goal: Increase Areal Densities beyond 1 Tb/in^2

Idea: Instead of writing in circular tracks that are far apart, pack the tracks closer allowing for 2D-ISI and use sophisticated signal processing algorithms.

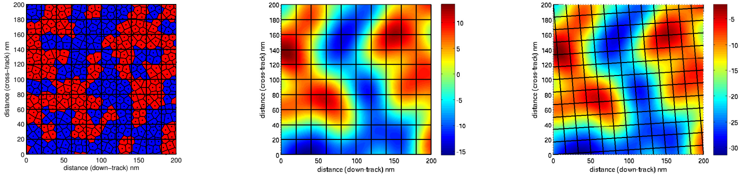

(a) Grains are magnetized according to the bit-values.

(b) Readback-signal is the sum of contributions from all grains.

(c) Non-ideal sampling with frequency offsets.

Figure : Voronoi-based granular media model.

TDMR Challenges

2D inter-symbol interference (2D ISI):

- 2D ISI detection in NP-hard.
- 2D coding techniques are generally 'difficult'.

Media Noise:

- Irregularities in sizes/positions of grains become prominent with decrease in bit-size.

2D Burst Erasures

- Traditional 1D ECCs are not suitable.

2D Timing and Synchronization Issues:

- Accurate timing is important with the reduction in bit-sizes.
- Frequency offsets in down-track direction due to timing errors in cross-track direction and vice-versa.

Others

- Read/write head design, suitable materials for the recording medium, etc.

2D Partial Response (PR) Equalization

Partial response (PR) equalization: Combined advantage of

- Low-complexity equalization.
- Performance of the ML detector.

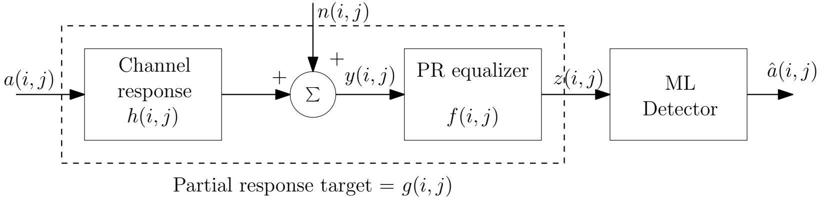

Figure : Combined response of the channel and the PR equalizer is approximated as PR target.

Our contributions:

- Extending 1D techniques to design 2D PR targets
  - unit energy and monic constraints.
- Design of separable and non-separable 2D PR targets to aid 2D ISI detection.

2D Soft-Output Viterbi Algorithm

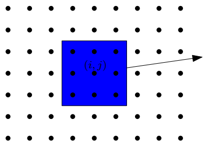

3×3 local span $\mathbf{M}$ of interpolated samples used for ML metric computation.

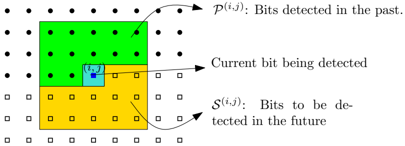

5×5 local span of bits used for ML metric computation. 12 of these samples are detected in the past and 12 will be detected in future.

- Locally optimal surface based detector.
- Operates in raster scan order.
- **2D Soft-output Viterbi algorithm:**
  - Maximizes likelihood probability of a local span ($\boldsymbol{M}$) of $y_{i,j}$:

$$\hat{x}_{i,j} = \arg\max_{\underline{x}} p\left(\underline{y}_{\boldsymbol{M}}^{(i,j)} \mid \underline{a}\right)$$

  - Equivalently, minimizes the ML metric given by:

$$\Gamma_{i,j}\left(\underline{x}\right) = \left\| \underline{y}_{\boldsymbol{M}}^{(i,j)} - \underline{\hat{y}}_{\boldsymbol{M}}^{(i,j)} \right\|^2,$$

    where $\hat{y}_{i,j} = \underline{g}^T \underline{a}_{\boldsymbol{G}}^{(i,j)}$ are the ideal-samples.
  - Soft-outputs: Using alternate ML metric corresponding to the wrong decision.

$$LLR_{i,j} = \min_{\underline{a}, a_{i,j}=-1} \Gamma_{i,j}\left(\underline{x}\right) - \min_{\underline{a}, a_{i,j}=1} \Gamma_{i,j}\left(\underline{a}\right).$$

2D SOVA with Timing Error Detection

Idea: Include timing information in the definition of ML metric.

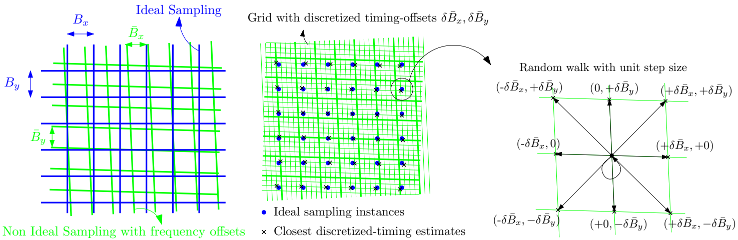

- The ideal sampling locations are approximated by discretizing the timing locations.
  - Using a finer grid with discrete offsets $\delta\bar{B}_x$ and $\delta\bar{B}_y$.
  - $\delta\bar{B}_x$ and $\delta\bar{B}_y$ are factors of non-ideal sampling intervals $\bar{B}_x$ and $\bar{B}_y$.
- Oversample the signal and interpolate to the estimated ideal sampling locations.
  - Optimal interpolation filters are designed using MMSE criterion.

ML Metric with Data-Dependent Noise Prediction

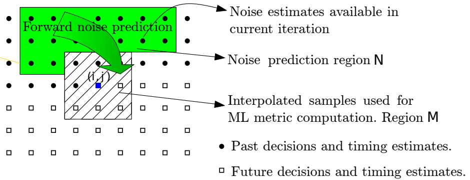

Figure : Noise prediction can be done to reduce the effect of media noise.

- Media noise is prominent in TDMR
  - Arises from the irregular bit-boundaries $\Longrightarrow$ correlated and pattern dependent.
- Correlated media noise has to be whitened for computing ML metric.
- Effect of media noise can be reduced by noise prediction using neighborhood noise samples.
- The updated ML metric with DDNP is given by

$$\Gamma_{\boldsymbol{i},\boldsymbol{j}}\left(\hat{a}\left(\mathcal{P}^{(\boldsymbol{i},\boldsymbol{j})}\right), a_{\boldsymbol{i},\boldsymbol{j}}, a\left(\mathcal{S}^{(\boldsymbol{i},\boldsymbol{j})}\right), \delta_{\underline{\mathcal{T}}}(i,j)\right)$$

$$= \left\|\left(\underline{\hat{e}}_{\boldsymbol{M}} - \underline{\mu}_{\boldsymbol{M}}(k)\right)\boldsymbol{W}(\mathrm{k}) - \left(\underline{\hat{e}}_{\boldsymbol{N}} - \underline{\mu}_{\boldsymbol{N}}(k)\right)\boldsymbol{P}(k)\right\|^{\boldsymbol{2}},$$

where

- $\hat{e}_{i,j} = \tilde{y}_{i,j} - \underline{g}^{\boldsymbol{T}}\underline{a}_{\boldsymbol{G}}^{(i,j)}$ are noise samples, $\boldsymbol{W}(k)$ and $\boldsymbol{P}(k)$ are noise-whitening and prediction filters.

Iterative 2D Timing Recovery Algorithm

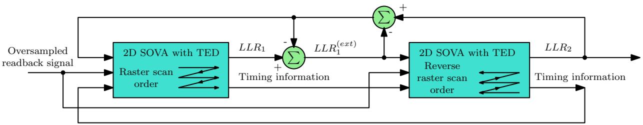

Figure : Two instances of 2D SOVA-TED operating in a turbo loop. The two instances exchange timing and bit-decision information with each other.

Idea: Use two instances of joint 2D timing recovery and signal detection algorithm in a turbo loop

1. Iteratively improve the timing estimates and bit-decisions.
2. Backward noise-prediction can be done using noise samples from previous iteration.

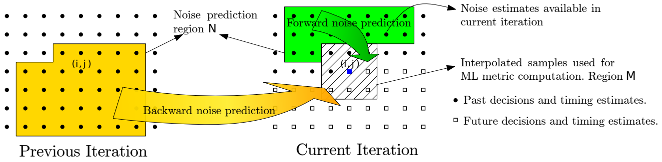

Figure : 7×7 noise prediction region N. Backward noise prediction can be done using noise estimates from previous iteration in a closed-loop configuration.

Simulation Results

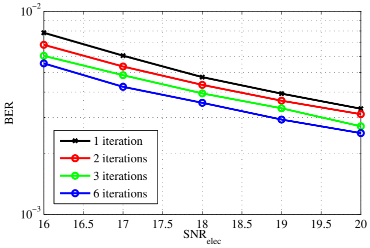

(a) CONFIG1: Raw-BER vs SNR in a closed-loop configuration.

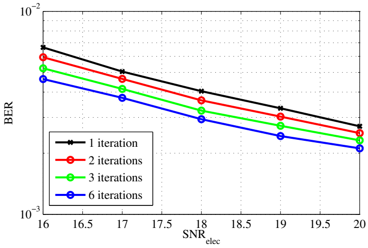

(b) CONFIG2: Raw-BER vs SNR in a closed-loop configuration.

- $>$ 1.2 dB SNR gain using turbo-loop over open-loop configuration.
- Separable frequency offsets give better performance.
- Corresponds to 10% gain in areal density.

2D Defect Detection and Burst Erasure Correction

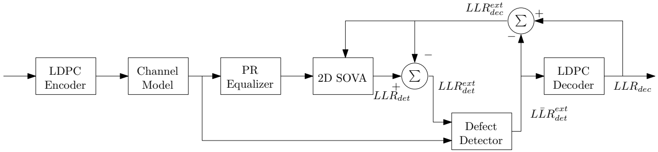

Figure : Defect detector indicates the estimated erasure locations to the LDPC decoder.

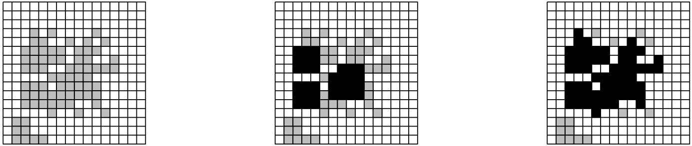

Figure : Defect detection algorithm: a) Potentially defective region is obtained using signal thresholding and defective patterns; b) Defective regions of at least 3×3 burst sizes are identified; c) Defective region is grown to include the potentially defective neighbors.

- Defective location is estimated using
  - Threshold on the signal level.
  - Defective patterns at the output of 2D SOVA.
- Belief propagation (BP) algorithm can correct erasures if the erasure locations are indicated.
- 2D SOVA and LDPC decoder operate in turbo loop to achieve further gains.

Defect Detector - Simulation Results

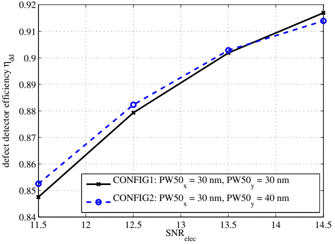

(a) Efficiency of the defect detector.

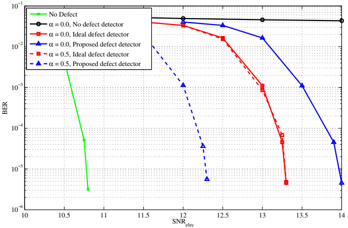

(b) BER performance of the burst erasure correction algorithm with 38x38 bursts.

- >90% efficiency of the defect detection algorithm as designed.
- Burst erasure correction with proposed algorithm
  - is within 0.5 dB of the performance of ideal defect detector for deep defects.
  - outperforms the ideal defect detector by 0.9 dB for shallow defects.

Summary

Summary:

- We have proposed a low complexity 2D signal detection algorithm:
  - 2D Separable and non-separable PR target design techniques.
  - 2D SOVA with data dependent noise prediction.
  - 1 patent filed on adaptive PR target design.
- We have proposed a joint iterative 2D timing recovery and signal detection algorithm
  - Iterative scheme to enable backward and forward noise prediction.
- We have proposed a method for 2D defect detection and burst erasure correction.

In progress:

- Closing on the exact analysis of 1D sequential detection algorithms.
- Analysis of 2D detection and timing recovery algorithms is in progress.

References

C. K. Matcha and S. G. Srinivasa, "Generalized Partial Response Equalization and Data Dependent Noise Predictive Signal Detection over Media Models for TDMR," *IEEE Trans. Magn.*, Oct. 2015.

——, "Defect Detection and Burst Erasure Correction for TDMR," *IEEE Trans. Magn.*, Nov. 2016.

——, "Joint Timing Recovery and Signal Detection for Two-Dimensional Magnetic Recording," *IEEE Trans. Magn.*, Feb. 2017.

——, "Joint Timing Recovery and Signal Detection for Two-Dimensional Magnetic Recording," *IEEE Trans. Magn.*, Feb. 2017.

B. P. Reddy, S. G. Srinivasa, and S. Dahandeh, "Timing Recovery Algorithms and Architectures for 2-D Magnetic Recording Systems," *IEEE Trans. Magn.*, Apr. 2015.

Y. Chen and S. G. Srinivasa, "Joint Self-Iterating Equalization and Detection for Two-Dimensional Intersymbol-Interference," *IEEE Trans. Comm.*, Aug. 2013.

Thank you!